

Ground and Excited State Intramolecular Proton Transfer in Salicylic Acid: an Ab Initio Electronic Structure Investigation

Shruti Maheshwari, Arindam Chowdhury,[†] and Narayanasami Sathyamurthy^{*,‡}

Department of Chemistry, Indian Institute of Technology, Kanpur 208016, India

Hirdyesh Mishra and H. B. Tripathi

Photophysics Laboratory, Department of Physics, Kumaun University, Nainital 263001, India

Manoranjan Panda and Jayaraman Chandrasekhar

Department of Organic Chemistry, Indian Institute of Science, Bangalore 560012, India

Received: April 12, 1999

Energetics of the ground and excited state intramolecular proton transfer in salicylic acid have been studied by ab initio molecular orbital calculations using the 6-31G** basis set at the restricted Hartree–Fock (RHF) and configuration interaction–single excitation (CIS) levels and also using the semiempirical method AM1 at the RHF level as well as with single and pair doubles excitation configuration interaction spanning eight frontier orbitals (PECI = 8). The ab initio potential energy profile for intramolecular proton transfer in the ground state reveals a single minimum corresponding to the primary form. In the first excited singlet state, however, there are two minima corresponding to the primary and tautomeric forms, separated by a barrier of ~6 kcal/mol, thus accounting for dual emission in salicylic acid. Electron density changes with electronic excitation and tautomerism indicate no zwitterion formation. Changes in spectral characteristics with change in pH, due to protonation and deprotonation of salicylic acid, are also accounted for, qualitatively. Although the AM1 calculations suggest a substantial barrier for proton transfer in the ground as well as the first excited state of SA, it predicts the transition wavelength in near quantitative accord with the experimental results for salicylic acid and its protonated and deprotonated forms.

1. Introduction

Excited state intramolecular proton transfer (ESIPT) in salicylic acid, its derivatives, and related systems has been the focus of attention of a large number of experimental and theoretical studies over the years. Weller,¹ in his pioneering work, had pointed out the dual emission in the fluorescence spectrum of salicylic acid and methyl salicylate and attributed it to asymmetric double well potentials arising from proton transfer in the ground state and also in the excited state, as shown schematically in Figure 1. The two wells in the ground state potential energy curve represent the primary (P) and tautomeric (T) forms, and the two wells in the excited state curve represent the corresponding excited states P* and T*, respectively. It is clear from the figure that the P form is the most stable in the ground state and T* in the excited state. Weller had also suggested that the excited state would be zwitterionic in nature.

The P form of salicylic acid (SA) involves an intramolecular hydrogen bond (IMHB), as shown in Figure 2. So does the T form, resulting from a proton transfer in P, accompanied by a reorganization of bonding electrons in the rest of the six-membered hydrogen bonded ring shown. It is important to point out here the possible existence of a rotamer (R) of P, with a weaker intramolecular hydrogen bond (see Figure 2). Salicylic acid is known to exist as a dimer in the solid state, in certain nonpolar solvents, and also in gas phase under moderate and

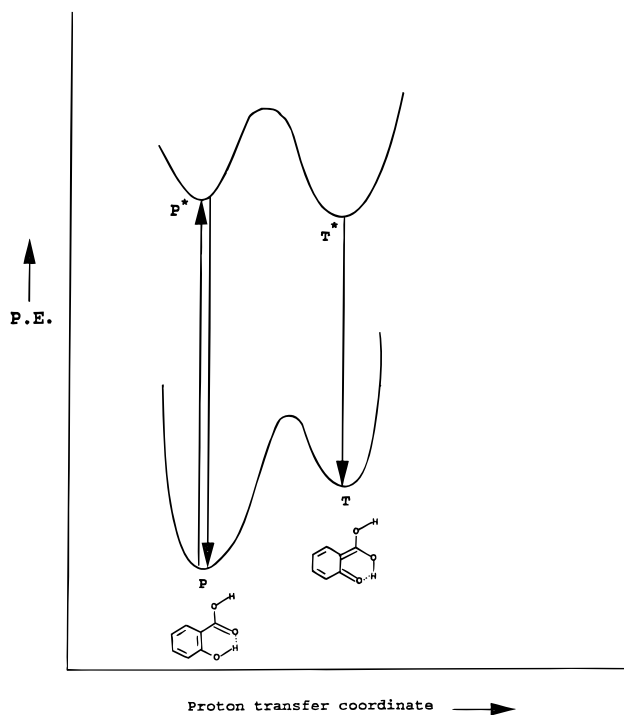


Figure 1. Schematic diagram of asymmetric double well potentials proposed by Weller¹ for the ground and excited states of salicylic acid.

high concentrations.^{2–5} It exists as a monomer in polar solvents⁶ and gets protonated and deprotonated depending upon the pH.⁷ As a result, the features of the emission spectrum of salicylic

[†] Present address: Department of Chemistry, Carnegie-Mellon University, Pittsburgh, Pennsylvania 15213.

[‡] Honorary Professor, S. N. Bose National Center for Basic Sciences, Calcutta, India.

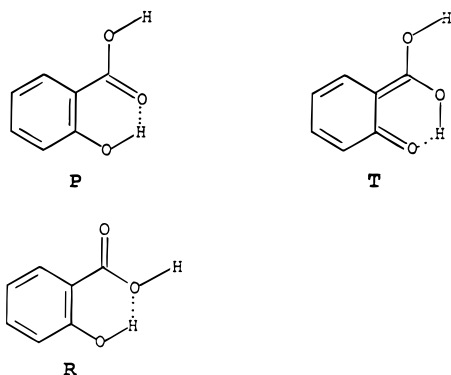


Figure 2. P, T, and R forms of salicylic acid.

acid are sensitive to the concentration of the solute and the solvent composition and shed light into the photophysics and photochemistry of salicylic acid.⁷

Bisht et al.⁵ had examined the excitation spectra of SA (monomer) under supersonic nozzle expansion conditions and concluded that there exist both the P and R forms in the ground state. They found the S_0 – S_1 transition to have its origin at 335.34 nm for P and 311.52 nm for R. They assigned them to π – π^* and n – π^* transitions, respectively. The P form emitted in the UV (340–370 nm) as well as in blue (380–480 nm) region, while the R emitted only in UV. This was attributed to the existence of the tautomeric form for P in its excited state. They also interpreted the large Stokes shift in emission from P as the signature of tautomerization and the motion of heavy atoms in the excited state.

Although the crystal structure and molecular structure of SA were established long ago,^{8,9} detailed studies of its electronic structure were rather limited. Catalán and Fernandez-Alonso¹⁰ had examined the electronic structure of SA and computed the potential energy curve for the ground and excited state intramolecular proton transfer (GSIPT and ESIPT) using semiempirical methods CNDO/2 and INDO. They made use of the experimentally known geometry of SA and determined the relative stabilities of different conformers. They found the P form to be the most stable and the rotamer (R) to be less stable by about 1.8 kcal/mol. The other possible conformers were higher in energy. They found the strength of the intramolecular hydrogen bond to be 13.4 kcal/mol in the P form, and 10.9 kcal/mol in the R form, in accord with available experimental estimates.¹¹ The IMHB was found to be stronger (20.9 kcal/mol) in the deprotonated form than in the neutral. When it came to determining the potential energy (PE) profile for the proton transfer, their studies were inadequate. In addition to their studies being semiempirical in nature, because of the computational limitations at that time, they froze the geometry of SA except for the position of the H atom involved in the proton transfer. While the ground state PE curve had a single minimum as a function of the distance r_{O_d-H} between the donor oxygen and the hydrogen atom in the P form, the PE curve for the lowest excited singlet state, identified as corresponding to π – π^* transition, had a double minimum, with the T* being the most stable. Subsequent studies by Sánchez-Cabezudo et al.¹² for methyl salicylate and its derivatives using CNDO–CI and INDO methods revealed that the shape of the PE profile for proton transfer is sensitive to the choice of $r_{O_d \cdots O_a}$ (the distance between the donor and acceptor atoms). More recently, Catalán et al.¹³ have examined the PE curves for the GSIPT and ESIPT in 2-hydroxybenzoyl compounds ($C_6H_4(OH)COR$, R = –H, –Me, –OMe, and –NH₂) using hybrid Hartree–Fock (HF)/density functional theory (DFT) and configuration interaction–single

excitation (CIS) approaches and found that intramolecular proton transfer is accompanied by changes in $r_{O_d \cdots O_a}$. As a matter of fact, midway through the proton transfer, the $O_d \cdots O_a$ distance was found to contract before relaxing to the value in the T form. They found that there was a single minimum in favor of the P form in the ground state and a single minimum in favor of the T form in the excited state. They also concluded that the P→T conversion proceeds through a photoexcited proton transfer and not a hydrogen atom transfer, although the final form (T) has *no* zwitterion character. From a detailed investigation of proton transfer in *o*-hydroxyacetophenone, Vener and Scheiner¹⁴ concluded that the double well potential was an artifact of the Hartree–Fock calculation and that inclusion of electron correlation led to single well potentials for the ground state as well as the lowest excited singlet state. They also concluded that the photoinduced tautomerism is not the result of proton motion only but also that of the accompanying motion of the heavier atoms in the hydrogen bonded ring.

Surprisingly, no result of ab initio electronic structure calculation of salicylic acid was reported until we started our investigations. Recently, Humbert et al.¹⁵ have reported a DFT-based spectral assignment for SA, salicylate anion, and the bianion in aqueous solution. Sobolewski and Domcke¹⁶ have reported the results of their ab initio calculations at different levels of accuracy: HF, CIS, Møller–Plesset second-order perturbation theory (MP2), and complete-active-space multi-configuration perturbation theory of second order (CASPT2). They determined the geometry of SA in its ground state and also that of P and T forms and the transition state (TS) in the first excited singlet state. They reported the vertical excitation energies for the $\pi\pi^*$ and $n\pi^*$ transitions from the ground state and also the PE profile for the S_1 state (corresponding to the $\pi\pi^*$ transition) at different levels of accuracy. Based on the nearly quantitative agreement obtained between the computed (316 nm) and the observed (311–335 nm) absorption maximum (λ_{max}) for SA, they concluded that the CASPT2 method yielded the best results and that dynamical electron correlation was very important for the system. Nevertheless, they emphasized that the CASPT2 results were by no means converged and that they were perhaps overemphasizing the stability of S_1 .

There remained still the need to study the strength of the intramolecular hydrogen bond and the relative stability of the P and R forms and the influence of protonation and deprotonation of SA on its spectral characteristics. Therefore we have carried out extensive HF and CIS calculations on various aspects of GSIPT and ESIPT in SA and its protonated and deprotonated forms and compared the results with the available experimental results.

In addition to high level ab initio calculations, semiempirical methods offer an attractive alternative for studying potential energy surfaces in ground and excited states. Procedures such as the AM1 method¹⁷ allow examination of PE surfaces without geometric assumptions. With inclusion of limited configuration interaction, especially through the single and pair double excitation (PECI) procedure, spectral properties of several conjugated organic systems have been shown to be reliably reproduced.¹⁸ Therefore, we have determined the spectral properties of SA and its protonated and deprotonated species using AM1/PECI = 8. The results are reported and compared with experiment and other theoretical results in the following sections.

2. Results and Discussion

Geometries and Energetics. All ab initio calculations reported in this paper were carried out using the *Gaussian 94*

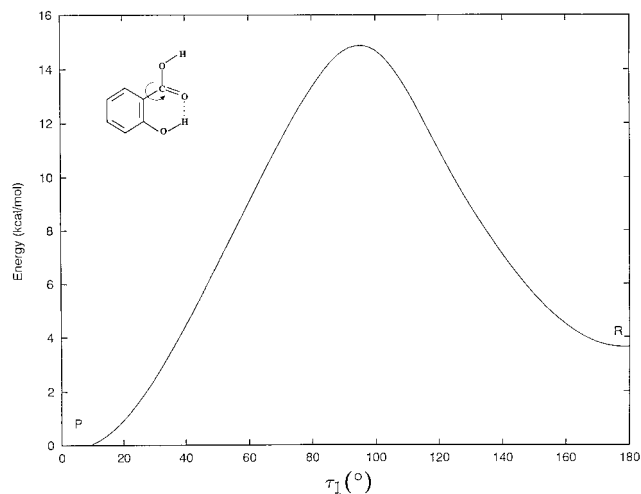


Figure 3. Energetics of the transformation from the P form to the R form of salicylic acid. For each value of τ_1 , the geometry has been optimized using the HF/6-31G** basis set.

TABLE 1: Relative Energies and Strengths of Intramolecular Hydrogen Bonds in Different Conformers of SA and Related Species in Their Ground Electronic States in kcal/mol Units

	DFT/B3LYP/		AM1		CNI-
	HF/ 6-31G**	6-31G**// AM1	RHF	PECI = 8	
Relative Stability					
SA (enol form, P)	0.0	0.0	0.0	0.0	0.0
SA (rotamer, R)	3.7	3.5	1.6	1.6	1.8
SA (keto form, T)	23.5	22.2	19.3	18.7	
Strength of Intramolecular Hydrogen Bond					
SA (enol form, P)	11.0	11.1	5.7	4.6	13.4
SA (rotamer, R)	6.6	7.8	3.9	3.0	10.9
SA (keto form, T)	27.7	18.8	9.4	10.6	
SA (+ H ⁺) (enol form, P)	2.5				
SA (- H ⁺) (enol form, P)	25.9	26.5	14.6	14.9	20.9

suite of programs.¹⁹ We compared the results for a number of different basis sets and found the HF/6-31G** to be the optimal basis set in terms of price–performance ratio for carrying out elaborate potential-energy curve investigations. The experimentally⁹ known geometry of salicylic acid (the P form) was reproduced by our calculations with a standard deviation of 0.08 Å for the distances and 1.8° for the angles. Here it must be added that the geometry of the T form was optimized, keeping the O_a –H distance the same as the O_d –H distance in the optimized geometry of the P form. Otherwise, optimization will lead to the P form! The P form is the most stable and the T form is 23.5 kcal/mol higher in energy. This is understandable because the proton transfer in P results in two –OH groups being bonded to an olefinic carbon atom in T, and also there is partial loss of aromaticity of the benzene ring, as suggested by Sobolewski and Domcke.²⁰

The R form is higher in energy than P by 3.7 kcal/mol, and the transformation from P to R involves rotation (τ_1) of the carboxylic acid group, with a barrier of 14.6 kcal/mol as shown in Figure 3. This is comparable to the known activation energy²¹ of ~10 kcal/mol.

DFT calculations using B3LYP functional at the 6-31G** basis set level (for the AM1 determined geometries) yield essentially the same relative stabilities for the P and T forms as obtained from ab initio calculations as shown in Table 1. AM1 calculations at restricted HF and PECI = 8 levels also yield comparable numbers.

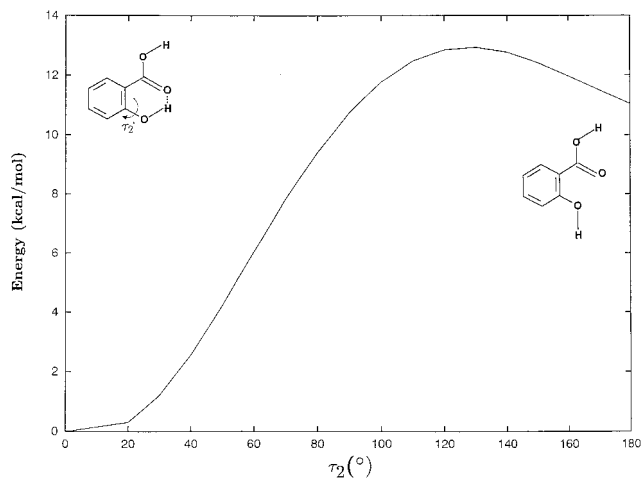


Figure 4. Energetics of the intramolecular hydrogen bond in the P form of SA. For each value of τ_2 , the geometry has been optimized using the HF/6-31G** basis set.

The strength of the intramolecular hydrogen bond in the P form was determined to be 11.0 kcal/mol by rotating the phenolic OH group out of the hydrogen bonded configuration and computing the difference in energy between the closed and open forms as shown in Figure 4. It may be noted that the barrier for phenolic OH rotation is 12.9 kcal/mol. The strength of the IMHB in T and R forms is 27.7 and 6.6 kcal/mol, respectively. The transformation from P to T in the ground electronic state can be thought of as arising from proton transfer from O_d to O_a , with concomitant redistribution of electron density in and around the six-membered hydrogen bonded ring. Alternatively, one could view this as a hydrogen atom transfer. In either case, one needs to identify the “reaction coordinate” and investigate the potential energy change along the reaction coordinate. Unfortunately, there does not seem to be any simple reaction coordinate definable for the system. It is tempting to consider stretching of the O_d –H bond distance and contracting of the H– O_a bond distance as constituting the reaction coordinate. Some authors have considered the $O_d \cdots O_a$ distance as fixed and varied the O_d –H bond distance. This may not be appropriate as it puts avoidable constraints on the system. Therefore we have chosen to vary r_{O_d-H} and optimize the rest of the structural parameters for each choice of r_{O_d-H} . This is sometimes referred to as the “distinguished-coordinate” approach in the literature.¹⁶ The resulting PE profile for the GSIPT, shown as a solid line in Figure 5, reveals that the P form is the most stable (as stated above). Surprisingly, there is no “well” for the T form. The barrier for the P to T transformation is substantial: 23.5 kcal/mol, large enough to make GSIPT unviable under thermal conditions. A plot of the $O_d \cdots O_a$ distance as a function of r_{O_d-H} in Figure 6(a) shows that as the proton transfer takes place, the $O_d \cdots O_a$ distance changes significantly. In the vicinity of a stable O_d –H bond, the $O_d \cdots O_a$ distance remains approximately constant. But as the proton moves farther away from O_d , $r_{O_d \cdots O_a}$ begins to contract before enlarging to a distance comparable to that in the T form. The $O_d \cdots H \cdots O_a$ angle also varies with r_{O_d-H} as shown in Figure 6(b). It enlarges during intramolecular proton transfer. Therefore it becomes clear that by freezing the geometry of salicylic acid or by fixing the $O_d \cdots O_a$ distance at a particular value, one ends up introducing artificial constraints on the system and hence a barrier for the P→T conversion.

Elsewhere, Vener and Schiener¹⁴ had pointed out that one has to include electron correlations and that ab initio calculations at the CI level lead to a single minimum in the ground state for

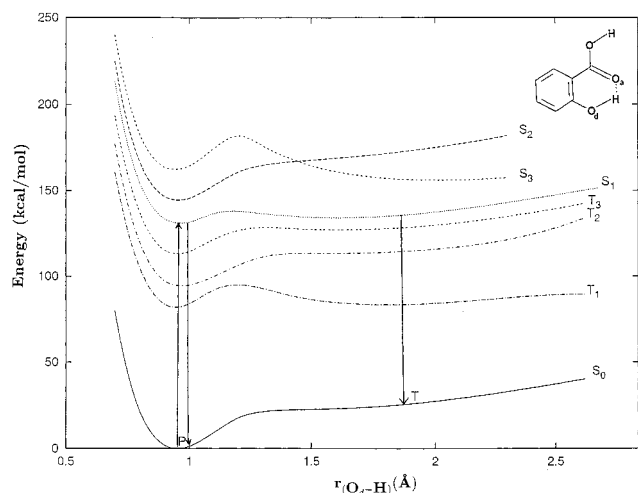


Figure 5. Potential energy profiles for intramolecular proton transfer in the ground state (S_0) of SA as obtained from HF/6-31G** calculations and for some of the excited states as obtained from a CIS calculation. The vertical arrows indicate the S_0 – S_1 absorption and dual emission.

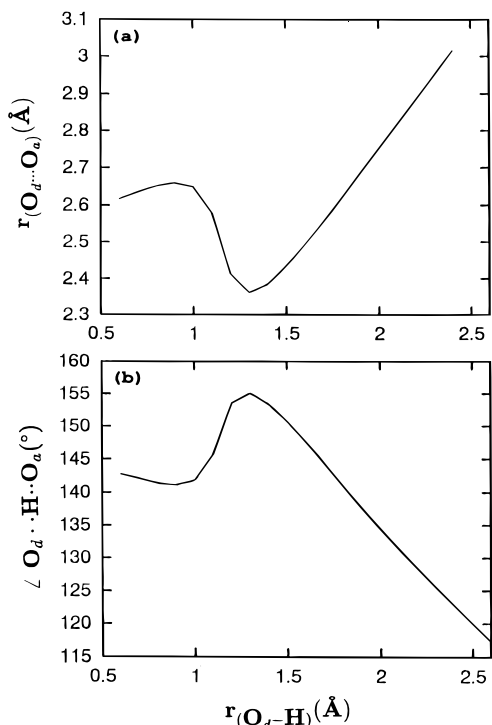


Figure 6. Variation of (a) the $O_d \cdots O_a$ distance and (b) $O_d \cdots H \cdots O_a$ angle with r_{O_d-H} , as obtained from the HF/6-31G** basis set calculations.

o-hydroxyacetophenone. Interestingly, for SA, even without including electron correlations, we have obtained a single minimum. The same conclusion has been arrived at by Sobolewski and Domcke.¹⁷ They further found that by including electron correlation through a CASPT2 calculation also one obtains a single minimum for the S_0 state of SA. AM1 calculations lead to a double well potential with a substantial barrier in between at the RHF level as well as the PECI = 8 level calculation!

Since our primary aim is to understand the origin of dual emission from the excited state of salicylic acid, we have undertaken a CIS study of the ground and excited states of salicylic acid using the 6-31G** basis set and including three singlet and three triplet excited states. The resulting PE profiles are shown in Figure 5. Here we must add that the excited state

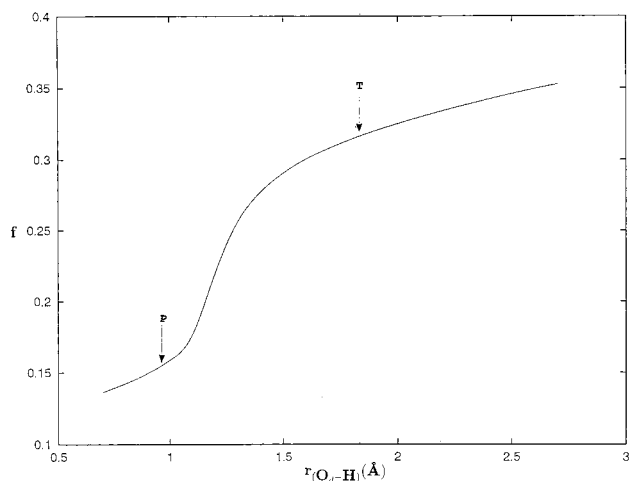


Figure 7. Oscillator strength (f) for the S_0 – S_1 transition of salicylic acid as a function of r_{O_d-H} .

PE curves have been obtained by adding the vertical excitation energies to the ground state energy at each geometry.

The absorption maximum (λ_{max}) for the P form works out to be 217.8 nm, when compared to the experimentally observed value of 311 nm for low concentrations of SA in cyclohexane.³ This discrepancy is not surprising because we have only carried out a CIS calculation. Although computing the ground state geometry of a molecular species using the LCAO–MO–SCF framework is more or less routine, computing the spectral properties is a daunting task. We hope that the qualitative features of the potential energy curves for the different electronic states obtained are still reliable.

It is clear from Figure 5 that the P form is the most stable in the lowest excited singlet (S_1) state also. Although there is a 6.8 kcal/mol barrier to proton transfer in S_1 , it must be pointed out that the PE curve is relatively shallow, indicating that emission from the excited state can take place over a range of wavelengths: 217.8–259.3 nm. Interestingly, the oscillator strength (f) for the S_0 – S_1 transition increases by a factor of 2 with increase in r_{O_d-H} as shown in Figure 7, indicating that the red-shifted emission can be substantial. While S_0 – S_1 and S_0 – S_2 transitions are of the π – π^* variety, S_0 – S_3 corresponds to n – π^* and the PE curve for S_3 has a marked double well behavior. The barrier (19.4 kcal/mol) for P→T conversion in S_3 is substantial, and T* is more stable than P*. The computed oscillator strength for the S_0 – S_3 transition is only ~ 0.0005 , while the experimental results suggest a strong n – π^* transition. Although there is no experimental evidence for the triplet states being involved in the dual emission of SA, we have included the PE curves for the three low lying triplet states in Figure 5.

The fact that there is dual emission in SA and its derivatives implies that there is sufficient time for geometrical changes to occur in the excited state. Therefore we have carried out geometry optimization for the S_1 state while varying r_{O_d-H} , and the results are shown in Figure 8, along with the vertical excitation energy results (see above). Qualitatively, the two curves are similar. But, quantitatively, there are differences. The adiabatic PE curve for S_1 is consistently lower than the vertical excitation energy curve, suggesting a larger Stokes shift for emission. The barrier for P*→T* conversion is also slightly lower (6.2 kcal/mol) on the adiabatic PE curve.

Charge densities on the atoms involved in ESAPT, computed using Mulliken population analysis, reveal that there is only a marginal change in the charges (O_d : $-0.66 \rightarrow -0.73$, H: $0.40 \rightarrow 0.43$ and O_a : $-0.64 \rightarrow -0.62$) in going from P→T*. This

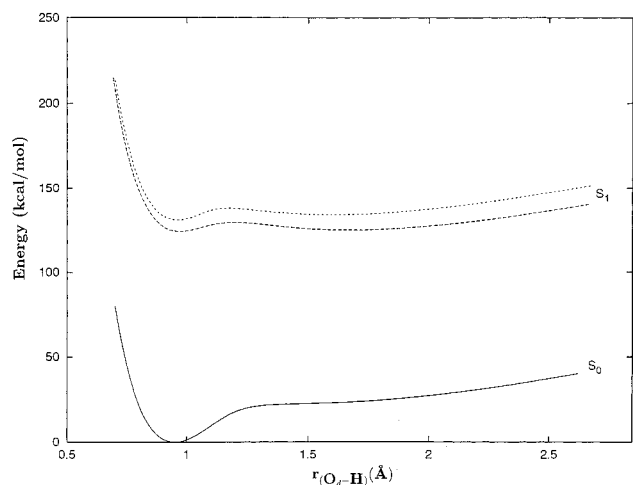


Figure 8. Adiabatic potential energy profile (for each value of $r_{\text{O-H}}$, the geometry of SA has been optimized) for intramolecular proton transfer in the S_1 state (---) and the corresponding vertical excitation energy curve (···). The ground state PE curve is included as a solid line for quick reference.

TABLE 2: Comparison of Spectral Characteristics (in nm units) for S_1 - S_0 Transition in Different Conformers of Salicylic Acid and Its Protonated and Deprotonated Forms

	Ab initio		Semiempirical	Exptl.
	CIS	CASPT2	AM1/ PECI = 8	
	Absorption Maxima (λ_{max})			
SA (enol form, P)	217.8 ^a	316 ^a	318.3 ^a	335.34 (gas) ⁵
	244.3 ^b		323.8 ^b	311 (cyclohexane) ³
SA (rotamer, R)	214.5 ^a		316.2 ^a	311.52 (gas) ⁵
SA(+H ⁺) (enol form, P)	236.4 ^b		390.9 ^a	328 (conc H ₂ SO ₄) ⁷
	261.5			329 (18 M H ₂ SO ₄) ⁶
SA(-H ⁺) (enol form, P)	208		292.9 ^a	295 (0.01 M NaOH) ⁶
				297 (MeOH + OH ⁻) ⁷
SA(-2H ⁺)	243.6		328.7 ^a	302 (6 N KOH) ⁷
				321 (7 N NaOH) ⁶
	Fluorescence Emission			
SA	217.8–259.3 ^a		318.3–379.2	340–370 (UV) ⁵
	244.3–310.4 ^b		323.8–486.2 ^b	380–480 (blue) ⁵
SA(-H ⁺)	208–243.3 ^a		292.9–354.9 ^a	405 ⁷

^a Vertical excitation. ^b Adiabatic.

means that there is change in polarity but *no* zwitterion formation following photoexcitation.

CIS calculations for the R form predict the λ_{max} to be 214.5 nm, when compared to the experimentally observed value of 311.5 nm in the gas phase.⁵ Analysis of the MOs involved in the transition suggest it to be π - π^* , same as for P, in contrast to the n - π^* assignment made in the literature.⁵ Since there is no likelihood of proton transfer in R, the PE curves have a single minimum in the ground and first excited singlet states (not shown).

Sobolewski and Domcke¹⁷ have shown that by including dynamic electron correlation through a CASPT2 calculation, they could predict λ_{max} (316 nm) for SA in agreement with experiment (see Table 2). Therefore we carried out AM1/PECI = 8 calculations that include single and pair double excitations

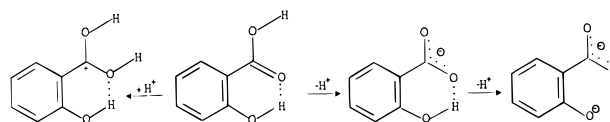


Figure 9. Scheme for protonation and deprotonation in salicylic acid with change in pH.

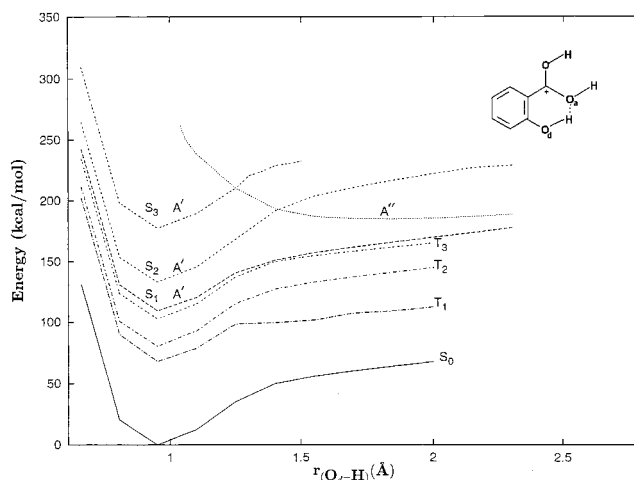


Figure 10. Potential energy profile for intramolecular proton transfer in the ground and excited states of salicylic acid in its protonated form as obtained from CIS calculations using the 6-31G** basis set.

and found that they also yield λ_{max} (318.3 nm) in agreement with experiment, as shown in Table 2.

Solvent and pH Effects. To account for the effect of solvent on the intramolecular proton transfer in SA, we have employed the self-consistent reaction field (SCRf) method, based on the Onsager reaction field model.²² In this model, the solute occupies a fixed spherical cavity of radius a_0 within the solvent field. A dipole in the molecule will induce a dipole in the medium, and the electric field applied by the solvent dipole will in turn interact with the molecular dipole, leading to a net stabilization. In the present work, a_0 , was taken to be 4.31 Å and the dielectric constant of the medium, ϵ , was chosen as 4.2 and 39.54, corresponding to diethyl ether and acetonitrile, respectively. The resulting ground and excited state PE curves are essentially identical to those obtained in the gas phase ($\epsilon = 1.0$) and hence are not shown.

With the addition of a mineral acid, SA gets protonated and with the addition of a base, it gets deprotonated, as illustrated in Figure 9. The PE profiles for intramolecular proton transfer in the protonated species, shown in Figure 10, reveal only a single well for the ground state and also for the lowest excited singlet (S_1) state. The lack of proton transfer is reinforced by a weak intramolecular hydrogen bond (~ 2.5 kcal/mol) in the protonated species. There are crossings between the PE profiles for the higher excited singlet states as shown in Figure 10. The λ_{max} computed for the $S_0 \rightarrow S_1$ transition is 261.5 nm when compared to 328 nm observed experimentally.⁷ Qualitatively, this means that the ab initio calculations are able to predict a red shift in λ_{max} due to protonation correctly. Interestingly the AM1/PECI = 8 calculations also suggest a red shift on protonation of SA, but much more than what is observed experimentally as can be seen from the spectral characteristics listed in Table 2.

As mentioned above, SA gets deprotonated with an increase in pH. But this can and does involve a stronger intramolecular hydrogen bond (25.9 kcal/mol). The PE profiles for the deprotonated species shown in Figure 11 reveal that the primary

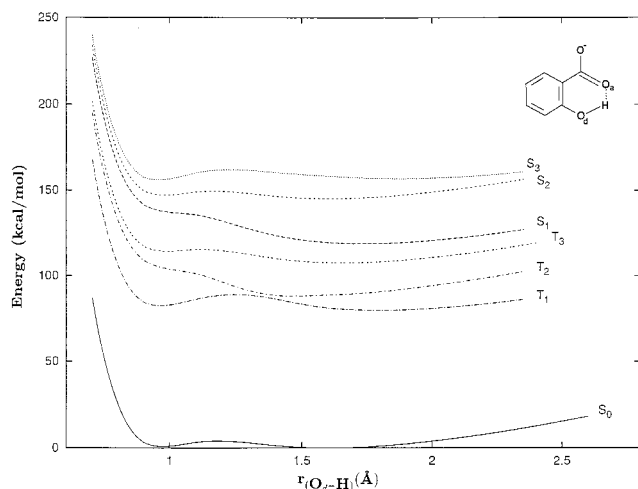


Figure 11. Potential energy profile for intramolecular proton transfer in the ground and excited states of salicylic acid in its deprotonated form, as obtained from CIS calculations using the 6-31G** basis set.

form and the tautomeric form are equally stable, giving rise to a double well potential, in the ground state. In the excited state (S_1), however, the tautomeric form is more stable (by 19.6 kcal/mol) than the primary. Therefore, the asymmetric double well potentials proposed for SA by Weller seem to be more appropriate for the deprotonated SA. The λ_{\max} computed for the deprotonated species is 208 nm, when compared to 297 nm observed experimentally.⁷ Thus ab initio theory predicts correctly a blue shift with deprotonation. The AM1/PECI calculations yield a λ_{\max} (292.9 nm) in excellent agreement with the experimentally observed λ_{\max} (295–297 nm)!

At very high pH, SA loses both the acidic protons and the resulting dianion has a λ_{\max} = 243.6 nm, compared to 302 nm observed experimentally.⁷ Interestingly, AM1/PECI = 8 calculations also yield a red shift in λ_{\max} in going from the deprotonated to the double deprotonated species, but far more than what is found in experiments (see Table 2).

3. Summary and Conclusion

Ab initio electronic structure calculations for salicylic acid at HF and CIS levels using the 6-31G** basis set predict the P form to be the most stable. The R form is less stable and the T form still less. The PE profile for intramolecular proton transfer in the ground electronic state of SA has a single minimum, corresponding to the P form. This finding is in agreement with what has been obtained from a CASPT2 calculation¹⁶ suggesting that the ground state properties are not crucially dependent on the inclusion of electron correlation for SA. The first excited singlet state has two minima corresponding to P* and T*, separated by a barrier ~6 kcal/mol in the CIS description, while CASPT2 calculations suggest a single minimum. Although the quantitative prediction of λ_{\max} by a CASPT2 calculation¹⁶ for SA emphasizes the need to include dynamic electron correlation for the system, we must point out that our CIS calculations account for the dual emission qualitatively correctly. The CIS calculations also predict qualitatively correctly the changes in spectral characteristics with change in pH, as summarized in Table 2.

We have found that intramolecular proton transfer in SA is accompanied by changes in the $O_a \cdots O_a$ distance and the $O_a \cdots H \cdots O_a$ angle, emphasizing the need to avoid freezing of geometries while investigating PE profiles. Our studies also show that while semiempirical calculations could predict ground state geometries, they could not be relied upon for detailed potential energy curve calculations and that they tend to introduce large barriers between tautomers. However, it must be emphasized that AM1/PECI = 8 calculations yield λ_{\max} in excellent agreement with experiment for SA and its protonated and deprotonated species.

Acknowledgment. We are grateful to Drs. S. K. Dogra and S. Manogaran for their valuable advice and assistance in various stages of this work. We are indebted to Dr. G. Madhavi Sastry for letting us use her MOPLLOT95 software. This study was supported in part by a grant from the Department of Science and Technology, New Delhi. S.M. and M.P. are grateful to CSIR, New Delhi for their fellowship.

References and Notes

- (1) Weller, A. Z. *Elektrochem.* **1956**, *60*, 1144; *Prog. React. Kinet.* **1961**, *1*, 187.
- (2) Joshi, H. C.; Tripathi, H. B.; Pant, T. C.; Pant, D. D. *Chem. Phys. Lett.* **1990**, *173*, 83.
- (3) Pant, D. D.; Joshi, H. C.; Bisht, P. B.; Tripathi, H. B. *Chem. Phys.* **1994**, *185*, 137.
- (4) Bisht, P. B.; Tripathi, H. B.; Pant, D. D. *J. Photochem. Photobiol. A: Chem.* **1995**, *90*, 103.
- (5) Bisht, P. B.; Petek, H.; Yoshihara, K.; Nagashima, U. *J. Chem. Phys.* **1995**, *103*, 5290.
- (6) Kovi, P. J.; Miller, C. L.; Schulman, S. G. *Anal. Chim. Acta* **1972**, *61*, 7.
- (7) Joshi, H. C.; Mishra, H.; Tripathi, H. B. *J. Photochem. Photobiol. A: Chem.* **1997**, *105*, 15.
- (8) Cochran, W. *Acta Crystallogr.* **1953**, *6*, 20.
- (9) Sundaralingam, M.; Jensen, L. H. *Acta Crystallogr.* **1965**, *18*, 1053.
- (10) Catalán, J.; Fernandez-Alonso, J. I. *Chem. Phys. Lett.* **1973**, *18*, 37; *J. Mol. Struct.* **1975**, *27*, 59.
- (11) Kolthoff, J. M.; Chantooni, M. K., Jr. *J. Am. Chem. Soc.* **1971**, *93*, 3843.
- (12) Sánchez-Cabezudo, M.; De Paz, J. L. G.; Catalán, J. *J. Mol. Struct.* **1985**, *131*, 277.
- (13) Catalán, J.; Palomar, J.; De Paz, J. L. G. *J. Phys. Chem. A* **1997**, *101*, 7914; *Chem. Phys. Lett.* **1997**, *269*, 151.
- (14) Vener, M. V.; Scheiner, S. *J. Phys. Chem.* **1995**, *99*, 642.
- (15) Humbert, B.; Alnot, M.; Quilès, F. *Spectrochim. Acta A* **1998**, *54*, 465.
- (16) Sobolewski, A. L.; Domcke, W. *Chem. Phys.* **1998**, *232*, 257.
- (17) Dewar, M. J. S.; Zebisch, E. G.; Healy, E. F.; Stewart, J. J. P. *J. Am. Chem. Soc.* **1985**, *107*, 3902.
- (18) Clark, T.; Chandrasekhar, J. *Israel J. Chem.* **1993**, *33*, 435. Jain, M.; Chandrasekhar, J. *J. Phys. Chem.* **1993**, *97*, 4044. Mitra, S.; Das, R.; Bhattacharyya, S. P.; Mukherjee, S. *J. Phys. Chem. A* **1997**, *101*, 293.
- (19) *Gaussian 94*, Revision C.2; Frisch, M. J.; Trucks, G. W.; Schlegel, H. B.; Gill, P. M. W.; Johnson, B. G.; Robb, M. A.; Cheeseman, J. R.; Keith, T.; Petersson, G. A.; Montgomery, J. A.; Raghavachari, K.; Al-Laham, M. A.; Zakrzewski, V. G.; Ortiz, J. V.; Foresman, J. B.; Cioslowski, J.; Stefanov, B. B.; Nanayakkara, A.; Challacombe, M.; Peng, C. Y.; Ayala, P. Y.; Chen, W.; Wong, M. W.; Andres, J. L.; Replogle, E. S.; Gomperts, R.; Martin, R. L.; Fox, D. J.; Binkley, J. S.; Defrees, D. J.; Baker, J.; Stewart, J. P.; Head-Gordon, M.; Gonzalez, C.; Pople, J. A. Gaussian Inc.: Pittsburgh, PA, 1995.
- (20) Sobolewski, A. L.; Domcke, W. *Chem. Phys.* **1994**, *184*, 115.
- (21) Sandros, K. *Acta Chem. Scand., Ser. A* **1976**, *30*, 761.
- (22) Onsager, L. *J. Am. Chem. Soc.* **1938**, *58*, 1486.